BIOMOLECULES & THERAPEUTICS

Original Article
Biomol Ther 29(5), 498-505 (2021)

Change in Cationic Amino Acid Transport System and Effect of Lysine Pretreatment on Inflammatory State in Amyotrophic Lateral Sclerosis Cell Model

Sana Latif and Young-Sook Kang*

College of Pharmacy and Drug Information Research Institute, Sookmyung Women's University, Seoul 04310, Republic of Korea

Abstract

Amyotrophic lateral sclerosis (ALS) is a lethal neurological disorder characterized by the deterioration of motor neurons. The aim of this study was to investigate alteration of cationic amino acid transporter (CAT-1) activity in the transport of lysine and the pretreatment effect of lysine on pro-inflammatory states in an amyotrophic lateral sclerosis cell line. The mRNA expression of cationic amino acid transporter 1 was lower in NSC-34/hSOD1^{G93A} (MT) than the control cell line (WT), lysine transport is mediated by CAT-1 in NSC-34 cell lines. The uptake of [^{3}H]L-lysine was Na^+-independent, voltage-sensitive, and strongly inhibited by inhibitors and substrates of cationic amino acid transporter 1 (system y^+). The transport process involved two saturable processes in both cell lines. In the MT cell line, at a high-affinity site, the affinity was 9.4-fold higher and capacity 24-fold lower than that in the WT; at a low-affinity site, the capacity was 2.3-fold lower than that in the WT cell line. Donepezil and verapamil competitively inhibited [^{3}H]L-lysine uptake in the NSC-34 cell lines. Pretreatment with pro-inflammatory cytokines decreased the uptake of [^{3}H]L-lysine and mRNA expression levels in both cell lines; however, the addition of L-lysine restored the transport activity in the MT cell lines. L-Lysine exhibited neuroprotective effects against pro-inflammatory states in the ALS disease model cell lines. In conclusion, studying the alteration in the expression of transporters and characteristics of lysine transport in ALS can lead to the development of new therapies for neurodegenerative diseases.

Key Words: Amyotrophic lateral sclerosis, NSC-34 cell lines, L-Lysine, Motor neuron disease, Cationic amino acid transporter 1

INTRODUCTION

Amyotrophic lateral sclerosis (ALS) is a terminal neurodegenerative disorder of motor neurons in the cortex, brainstem, and spinal cord (Jung *et al*., 2013). Most ALS cases are sporadic, and up to 5-10% of cases are familial. Missense mutations of Cu/Zn superoxide dismutase (SOD1) cause approximately 25% of familial ALS cases, whose pathological and clinical features are incomprehensible compared to those of sporadic ALS (Rojas *et al*., 2015). The precise molecular pathways causing the death of motor neurons in ALS remain unclear. Nonetheless, possible changes in the affected motor neurons include disorganization of intermediate filaments, protein aggregation, glutamate-mediated excitotoxicity, nitroxidative stress from reactive oxygen species (ROS), and intracellular calcium dysregulation (Rowland and Shneider, 2001). Amino acids play an essential role in the CNS as neurotransmitters, neuromodulators, and regulators of metabolism (Wee *et al*., 2013; Adachi *et al*., 2018).

Transport of cationic amino acids (CAAs), including lysine, arginine, and ornithine, is conducted by two protein families that are present in various tissues: cationic amino acid transporter (CAT), referred to as system y^+, and broad-scope amino acid transporters (Bat), which comprises system $b^{0,+}$, $B^{0,+}$, and y^+L (O'Kane *et al*., 2006). System y^+L was first identified in human erythrocytes (Devés *et al*., 1993). System $B^{0,+}$ is a Na^+-dependent transport system present in human epithelial cells that transports CAA, as well as neutral amino acids (NAA) (Van Winkle *et al*., 1990; Bahri *et al*., 2008). System $b^{0,+}$, a facilitative transporter, has also been associated with the transport of CAA in proximal tubular cells (Mitsuoka *et al*., 2009) and mouse blastocysts (Furesz *et al*., 1991). Lysine with its lysyl ($(CH_2)_4NH_2$) side chain is a positively charged and basic amino acid at physiological pH. It influences the function of proteins involved in the development, cell–cell interaction, signal transduction, and several other biological processes

Open Access **https://doi.org/10.4062/biomolther.2021.037**

Received Feb 19, 2021 **Revised** Mar 31, 2021 **Accepted** Apr 2, 2021
Published Online May 3, 2021

***Corresponding Author**
E-mail: yskang@sm.ac.kr
Tel: +82-2-710-9562, Fax: +82-2-710-9871

(Ukmar-Godec *et al*., 2019). Previous studies have shown that the acylation of lysine residues in SOD1 decreases its rate of nucleation and elongation into amyloid-like fibrils that are linked to ALS (Rasouli *et al*., 2017). *In vivo* experiments indicate that system y^+ is the primary mechanism for CAA transport across the blood–brain barrier (BBB) in a Na^+-independent manner (Closs *et al*., 2004). However, lysine transport in the NSC-34 cell line has not been elucidated; therefore, in the present study, we aimed to identify the transporter(s) involved in the transport of lysine in an ALS cell-line model.

Furthermore, as reported earlier, the levels of free amino acids were altered in the lumbar spinal cord of ALS mice compared to that in WT mice (Jung *et al*., 2013). In this regard, it was previously demonstrated that the uptake of serine was decreased in the mutant-type (MT) cell line NSC34/hSOD1^{G93A} compared to that in the control [wild type; WT (NSC34/hSOD-1^{wt})] cell lines of ALS. In contrast, L-serine uptake was increased in the MT cell lines and decreased in the WT cell lines (Lee *et al*., 2017). In addition, the uptake of [^{14}C] L-citrulline, a neutral amino acid, was lower in the ALS model (MT) than in the WT (Gyawali *et al*., 2021). In an earlier study, abnormal levels of basic amino acids, including lysine and other essential amino acids, were reported to be elevated in the CSF of patients with ALS (Patten *et al*., 1978; Iłzecka *et al*., 2003). The relevance of L-lysine in ALS was indicated by the observation that its levels were elevated in the lumbar spinal cord of mutant SOD1^{G93A} mice than in the lumbar spinal cord of control mice (Jung *et al*., 2013).

The characteristics of L-lysine transport across the ALS cell lines remain unclear. Therefore, the objective of this study was to investigate the expression of the CAA transporter system using real-time polymerase chain reaction (PCR) analysis and to study the characteristics of L-lysine transport in the ALS cell line model. In addition, we studied the effect of lysine under various pro-inflammatory states in the NSC-34 cell line.

MATERIALS AND METHODS

Radioisotope and chemicals

[^{3}H]L-Lysine (specific activity 91 Ci/mmol) was purchased from PerkinElmer (Boston, MA, USA). All other chemicals and reagents were of reagent grade.

Cell culture

Motor neuron-like cells (NSC-34, NSC-34/hSOD1^{wt} cell lines (WT) and NSC-34/hSOD1^{G93A} cell lines (MT), passages 10-19) were cultured using the protocols used in previous study (Cashman *et al*., 1992; Lee *et al*., 2017). NSC-34 cell lines were obtained from Prof. Hoon Ryu (KIST, Seoul, Korea), the cells were cultured in Dulbecco's modified Eagle's medium (DMEM; HyClone, UT, USA) supplemented with 10% fetal bovine serum (Mediatech, Woodland, CA, USA), 100 U/mL penicillin, and 100 μg/mL streptomycin. These cells were maintained in a humidified atmosphere of 5% CO_2/air at 37°C. The NSC-34 cell lines (1×10^5 cells/well) were seeded on rat tail collagen type I-coated 24-well culture plates (Biocoat, Kennebunk, ME, USA). After 48 h of incubation at 37°C, the cells became confluent; subsequently, they were used for the uptake study.

Real-time PCR

Total RNA was isolated from cultured cells using the RNeasy Mini kit (250) from Qiagen (Valencia, CA, USA) according to the manufacturer's instructions. After isolation, the RNA was stored at −20°C, and the concentration and purity of the RNA was determined by measuring the absorbance at 260 and 280 nm using a spectrophotometer. Total RNA (2 μg) was reverse-transcribed using a high-capacity cDNA reverse transcription kit (Applied Biosystems, V.A. Graiciuno, Lithuania). Quantitative real-time PCR analysis was performed using the TaqMan® Gene Expression Master Mix (Applied Biosystems) and StepOne real-time PCR system (Applied Biosystems, Foster City, CA, USA), according to the manufacturer's protocols (Gyawali *et al*., 2021). GAPDH was used as an internal control. The results were analyzed using the StepOnePlus software (Applied Biosystems) and expressed as Ct, the threshold cycle for target amplification (Lee *et al*., 2017).

Slc7a1/system y^+ small interfering RNA (siRNA) and control siRNA transfection

Transient knockdown of CAT-1/Slc7a1 (system y^+) in the NSC-34 cell lines was achieved using an siRNA from Dharmacon (Dharmacon Inc. Lafayette, CO, USA). Slc7a1 was targeted with a smart pool containing siRNA. The final concentration was 100 nM. Slc7a1 and the control siRNA were delivered to the NSC-34 cells using Lipofectamine 2000 (Invitrogen, Carlsbad, CA, USA) in accordance with the manufacturer's protocol. The cells were used 24 h after the initiation of transfection for the evaluation of [^{3}H]L-lysine uptake and quantitative real-time PCR analysis (Lee and Kang, 2016).

[^{3}H]L-Lysine uptake study in NSC-34 cell lines

The uptake study for [^{3}H]L-lysine was performed according to a previously described procedure (Gyawali *et al*., 2021). Briefly, extracellular fluid buffer (ECF) containing [^{3}H]L-lysine (0.5 μCi/well, 27 nM) in the presence or absence of unlabeled inhibitors was added to the NSC-34 cell lines and incubated at 37°C and pH 7.4 for 5 min. An ice-cold ECF buffer was used to terminate the uptake process. To prepare an Na^+-free transport medium, sodium chloride was replaced with lithium chloride and choline chloride, and sodium bicarbonate was replaced with potassium bicarbonate. Membrane potential depletion media were prepared by replacing sodium chloride and sodium bicarbonate with potassium chloride and potassium bicarbonate, respectively. In addition, 10 μM valinomycin was dissolved in the transport buffer and preincubated with the cells for 10 min, followed by uptake (Gyawali and Kang, 2019). The cells were solubilized with 750 μL of 1 N NaOH in PBS through overnight incubation at room temperature, and radioactivity was measured using the LS 6500 scintillation counter (Beckman, Fullerton, CA, USA).

The cell-to-medium ratio (μL/mg protein) was calculated as follows: cell-to-medium ratio (μL/mg protein)=([^{3}H]dpm in the cell/amount (mg) of the protein)/([^{3}H]dpm in the medium/amount (μL) of medium)×100.

Data analysis

In kinetic studies, the Michaelis–Menten constant (K_m) and the maximum uptake rate (V_{max}) of [^{3}H]L-lysine was estimated using the following equation:

$$V=[V_{max1}\times C/(K_{m1}+C)+K_{ns1}\times C]+[V_{max2}\times C/(K_{m2}+C)+K_{ns2}\times C], \quad (1)$$

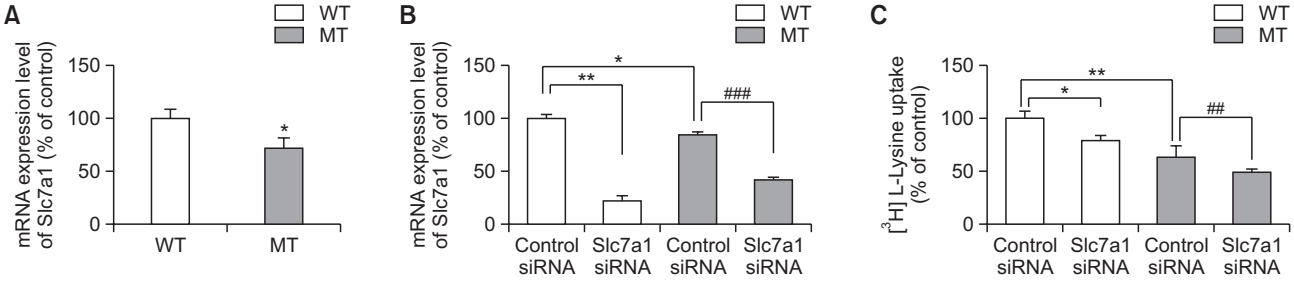

Fig. 1. mRNA expression and effect of Slc7a1 siRNA in NSC-34 cell lines. (A) Slc7a1/system y^+ mRNA expression. (B) Effect of Slc7a1 siRNA on the mRNA expression, as determined using quantitative RT-PCR analysis and normalized to the mRNA expression of GAPDH. (C) [^{3}H]L-lysine uptake after Slc7a1 siRNA transfection was performed at pH 7.4 and 37°C for 5 min. Each value represents the mean ± SEM. (n=3-4). *p<0.05, **p<0.01, $^{\#\#}p$<0.01, $^{\#\#\#}p$<0.001 indicate significant difference with respect to the control.

where C is the concentration of lysine, and V_{max1} and V_{max2} are the maximum uptake rates for high-affinity and low-affinity processes, respectively. K_{m1} is the Michaelis–Menten constant for the high-affinity process, and K_{m2} is the Michaelis–Menten constant for the low-affinity process. K_{ns1} and K_{ns2} are the first-order constants for the non-saturable components in the high-affinity and low-affinity processes, respectively (Gyawali and Kang, 2021b).

Following statistical analysis, all data in the figures were presented as the mean ± standard error of the mean (SEM). The data were analyzed using one-way analysis of variance (ANOVA) with Dunnett's post-hoc test. A sigma plot was used for plotting figures and bar charts. A comparison of the two groups was performed using a two-tailed unpaired t-test. p values<0.05 were considered statistically significant.

RESULTS

The mRNA expression level of CAT1 and effect of CAT1 (Slc7a1) siRNA on mRNA expression and uptake of [^{3}H] L-lysine in NSC-34 cell lines

The mRNA expression levels of CAT1 (Slc7a1) were measured using real-time PCR analysis in the NSC-34 cell lines. The relative gene expression of Slc7a1 was lower in the NSC-34/hSOD1^{G93A}, which serves as a disease model cell line of ALS (MT), than in the NSC-34/hSOD1^{wt} cell line, which serves as the control cell line (WT) (Fig. 1A). To confirm whether Slc7a1/system y^+ was involved in the uptake of [^{3}H]L-lysine in the ALS cell line model, Slc7a1 knockdown via siRNA transfection was performed in both NSC-34 cell lines. The mRNA levels of the Slc7a1 siRNA were significantly reduced in the NSC-34 cell lines compared to that of the control siRNA, as analyzed by quantitative real-time PCR (Fig. 1B). Additionally, [^{3}H]L-lysine uptake was significantly reduced in both NSC-34 cell lines transfected with siRNA compared to that in the cells transfected with the control pool siRNA (Fig. 1C). Altogether, our findings suggest the involvement of Slc7a1 in the transport of L-lysine in the NSC-34 cell lines.

Effect of ion dependency on [^{3}H]L-lysine uptake in NSC-34 cell lines

To determine whether [^{3}H]L-lysine uptake is sodium-dependent or sodium-independent, we performed an ion dependence study. No significant differences in [^{3}H]L-lysine uptake were observed upon replacement of sodium chloride with lithium chloride and choline chloride in the transport buffer. Moreover, disruption of the membrane potential gradient and valinomycin pretreatment induced a significant decrease in [^{3}H]L-lysine uptake in both WT and MT cell lines, as shown in Table 1. Our results indicate that [^{3}H] L-lysine uptake in the NSC-34 cell lines is sodium-independent and voltage-sensitive.

Table 1. Effect of sodium replacement and membrane potential on [^{3}H]L-lysine uptake by NSC-34 cell lines

Treatment	Relative uptake (% of control)	
	WT	MT
Control	100 ± 9	100 ± 2
Na^+ replacement		
Lithium chloride	110 ± 7	91.5 ± 1.0
Choline chloride	89.6 ± 1.7	95.0 ± 7.5
Membrane potential		
Valinomycin (10 μM)	68.9 ± 5.7*	53.8 ± 4.9***
Potassium chloride	72.8 ± 7.7**	59.6 ± 1.1***

[^{3}H]L-Lysine uptake by NSC-34 cell lines was performed at 37°C for 5 min at pH 7.4. Sodium containing extracellular fluid (ECF) buffer was replaced with lithium chloride and choline chloride (Na^+ free) to disrupt the sodium ion gradient and potassium chloride (KCl) to disrupt the membrane potential ion gradient. Each point represents the mean ± SEM (n=3-4). *p<0.05, **p<0.01, ***p<0.001 indicate significant difference with respect to the control.

Effect of several transporters on [^{3}H]L-lysine uptake by NSC-34 cell lines

Through inhibition studies, we assessed the effect of several transporter inhibitors to distinguish the transporter systems involved in L-lysine transport in the ALS cell-line model. [^{3}H] L-Lysine uptake was significantly inhibited by *N*-monomethyl-L-arginine (N-MMA), homoarginine, and *N*-ethylmaleimide (NEM), which are potent inhibitors of system y^+ in both cell lines. In addition, harmaline, which is an inhibitor of b^{0+}, significantly reduced the uptake of [^{3}H]L-lysine in the WT and MT cell lines. In contrast, [^{3}H]L-lysine uptake was not inhibited by 2-aminobicyclo-(2,2,1)-heptane-2-carboxylic acid (BCH), which is an inhibitor of system $B^{0,+}$ and the only Na^+-dependent carrier transport system that transports CAA with a low affinity for NAA in both NSC-34 cell lines, as shown in Table 2. However, no inhibition was observed with *N*-methylmaleimide

(N-MM), which is an inhibitor of system y^+L.

Characterization of [^{3}H]L-lysine transport in NSC-34 cell lines

To investigate the changes in the transport activity of L-lysine in NSC-34 cell lines, we performed uptake studies. The uptake of [^{3}H]L-lysine was increased in a time-dependent manner and was linear for 5 min. Therefore, in the subsequent kinetic and inhibition analyses, [^{3}H]L-lysine uptake by the ALS cell line was assessed at 5 min. The uptake of [^{3}H]L-lysine in the MT cell line was significantly lower than that in the WT cell line, as shown in Fig. 2A.

The kinetics of [^{3}H]L-lysine uptake in the NSC-34 cell lines were analyzed by examining the concentration dependence of [^{3}H]L-lysine uptake. The transport of [^{3}H]L-lysine was saturated in both cell lines (Fig. 2B, 2C); however, the uptake was lower in the MT cell line than in the WT. The Eadie–Hofstee plot (Fig. 2B, 2C, inset) shows two straight lines, indicating that two saturable processes are involved in the uptake of [^{3}H] L-lysine in the NSC-34 cell lines. According to the kinetic analysis, in the WT cell lines, at the high-affinity site, K_{m1}=0.062 ± 0.001 mM and V_{max1}=1.70 ± 0.26 (nmol/mg protein/min), and at the low-affinity site, K_{m2}=0.48 ± 0.08 mM and V_{max2}=8.48 ± 0.71 (nmol/mg protein/min). The corresponding values for the MT cell line were K_{m1}=0.0066 ± 0.0003 mM, K_{m2}=0.31 ± 0.14 mM, V_{max1}=0.072 ± 0.002 (nmol/mg protein/min), and V_{max2}=3.71 ± 0.88 (nmol/mg protein/min). These parameters indicate that L-lysine transport in the NSC-34 cell line involved a carrier-mediated transport system. At the high-affinity site, the affinity was 9.4-fold higher and the capacity was lower (4.2% of WT value) in the MT cell line compared to that in the WT cell line, and at the low-affinity site, the affinity was 1.5-fold higher and the capacity was (44% of WT value) lower than that in the WT cell line. The data obtained are shown in Table 3.

Table 2. Effect of several transporters on uptake of [^{3}H]L-lysine by NSC-34 cell lines

Substrates	Conc. (mM)	[^{3}H]L-Lysine uptake (% of control)	
		WT	MT
Control		100 ± 2	100 ± 2
+N-MMA	2	37.8 ± 2.1***	24.4 ± 0.3***
+Homoarginine	2	37.9 ± 2.7***	30.7 ± 2.3***
+NEM	2	63.4 ± 5.8***	79.7 ± 4.2***
+Harmaline	1	35.1 ± 6.8**	63.3 ± 6.4**
+BCH	2	90.6 ± 5.0	92.2 ± 5.8
+N-MM	2	100 ± 8	109 ± 5

[^{3}H]L-Lysine uptake by WT and MT cell lines was measured at 37°C for 5 min at pH 7.4, in the absence (control) or presence of 1-2 mM solutions of inhibitors. Each value represents the mean ± SEM (n=3-4). **p<0.01, ***p<0.001 indicate significant difference with respect to the control. N-MMA, N-monomethyl-L-arginine; NEM, N-ethylmaleimide; BCH, 2-aminobicyclo-(2,2,1)-heptane-2-carboxylic acid; N-MM, *N*-methylmaleimide.

Effect of various L-amino acids on [^{3}H]L-lysine uptake by NSC-34 cell lines

To study the effect of numerous amino acids on the L-lysine transport in ALS cell lines, [^{3}H] we measured the L-lysine uptake in the presence of 2 mM unlabeled L-amino acids. Uptake was significantly inhibited by CAA, including lysine, arginine, and ornithine, in the NSC-34 cell lines. Alanine, which is a substrate of the alanine–serine–cysteine (ASC) system, showed significant inhibition in both cell lines. In addition, leucine, glutamine, and histidine showed significant inhibition in the WT and MT cell lines. However, L-citrulline, a substrate of large

Table 3. Kinetic parameters of [^{3}H]L-lysine uptake in NSC-34 cell lines

Parameters	WT	MT
K_{m1} (mM)	0.062 ± 0.001	0.0066 ± 0.0003***
V_{max1} (nmol/mg protein/min)	1.70 ± 0.26	0.072 ± 0.002***
K_{m2} (mM)	0.48 ± 0.08	0.31 ± 0.14
V_{max2} (nmol/mg protein/min)	8.48 ± 0.71	3.71 ± 0.88**
K_{ns1} (μL/min mg protein)	5.69 ± 0.89	6.57 ± 0.04
K_{ns2} (μL/ min mg protein)	3.26 ± 0.78	2.95 ± 1.66

K_m, V_{max}, and K_{ns} are transport affinity, maximum transport velocity, and non-saturable transport clearance, respectively. **p<0.01, ***p<0.001 indicate significant difference with respect to the control (WT). Each value represents the mean ± SEM (n=3).

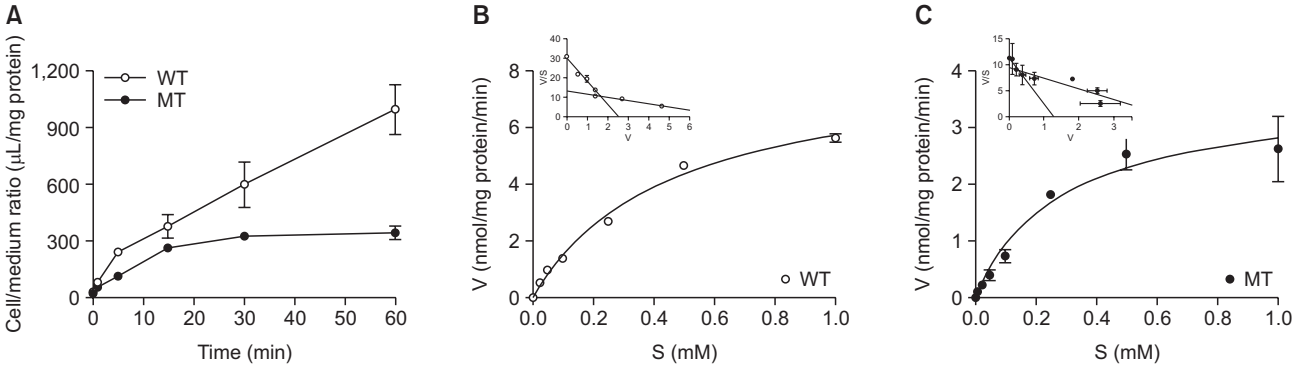

Fig. 2. Uptake of [^{3}H]L-lysine uptake in NSC-34 cell lines. (A) Time course of [^{3}H]L-lysine uptake by WT and MT cell lines. [^{3}H]L-lysine uptake was performed at pH 7.4 and 37°C for 0-60 min in ECF buffer. (B) Saturation kinetics of [^{3}H] L-lysine in WT cell line. (C) Saturation kinetics of [^{3}H]L-lysine in MT cell line. [^{3}H]L-Lysine uptake was performed with an incubation time of 5 min at pH 7.4 and 37°C in the presence of 0-1 mM unlabeled L-lysine. The insert data are presented as an Eadie–Hofstee plot. Each point represents the mean ± SEM (n=3-4).

Table 4. Effect of various L-amino acids on uptake of [^{3}H]L-lysine by NSC-34 cell lines

Substrates	Conc. (mM)	[^{3}H]L-Lysine uptake (% of control)	
		WT	MT
Control		100 ± 2	100 ± 5
+Lysine	2	26.2 ± 3.6**	16.4 ± 6.8***
+Ornithine	2	18.5 ± 1.8***	20.2 ± 0.7***
+Arginine	2	30.9 ± 3.2***	22.1 ± 3.0***
+Leucine	2	56.6 ± 3.0**	42.1 ± 4.4***
+Glutamine	2	87.8± 0.8***	48.2 ± 3.7***
+Histidine	2	79.3 ± 0.4**	73.6 ± 4.5**
+Alanine	2	77.6 ± 2.7***	76.4 ± 0.8***
+Citrulline	2	99.3 ± 10.8	108 ± 4
+Choline	2	90.7 ± 4.9	93.2 ± 0.6

[^{3}H]L-Lysine uptake by WT and MT cell lines was measured at 37°C for 5 min at pH 7.4, in the absence (control) or presence of 2 mM L-amino acids. Each value represents the mean ± SEM (n=3-4). **p<0.01, ***p<0.001 indicate significant difference with respect to the control.

Table 5. Effect of drugs on uptake of [^{3}H]L-lysine by NSC-34 cell lines

Substrates	Conc. (mM)	[^{3}H]L-Lysine uptake (% of control)	
		WT	MT
Control		100 ± 6	100 ± 4
+Quinidine	2	26.1 ± 4.6***	20.3 ± 1.3***
+Gabapentin	2	55.1 ± 2.3***	49.1 ± 1.9***
+Donepezil	2	59.4 ± 8.3*	50.7 ± 3.9*
+Verapamil	0.5	56.7 ± 5.4**	54.1 ± 2.6**
+Clonidine	2	51.7 ± 2.1***	57.8 ± 6.0**
+L-dopa	2	81.1 ± 5.0***	79.1 ± 6.4*
+Amiloride	2	111 ± 2	97.5 ± 8.9
+Paeonol	2	138 ± 9	109 ± 3
+Dopamine	2	122 ± 9	113 ± 8
+Riluzole	0.5	127 ± 8	125 ± 6
+Baclofen	2	102 ± 6	127 ± 10

[^{3}H]L-Lysine uptake by WT and MT cell lines was measured at 37°C for 5 min at pH 7.4, in the absence (control) or presence of 0.5-2 mM drug solutions. Each value represents the mean ± SEM (n=3-4). *p<0.05, **p<0.01, ***p<0.001 indicate significant difference with respect to the control.

neutral amino acid transporter 1 (LAT-1) did not inhibit [^{3}H] L-lysine uptake in either NSC-34 cell line, as shown in Table 4.

Effect of drugs on [^{3}H]L-lysine uptake by NSC-34 cell lines

We performed an uptake study to analyze the inhibitory effect of L-lysine and various drugs in the WT and MT cell lines. [^{3}H]L-Lysine uptake was strongly inhibited by verapamil, a substrate of organic cation transporter; donepezil hydrochloride, a drug used to treat Alzheimer's disease (AD); and quinidine. In addition, other drugs, including clonidine, gabapentin, and L-dopa significantly inhibited [^{3}H]L-lysine uptake in the WT and MT cell lines. However, no significant effect was observed with baclofen, which is a substrate of LAT-1, in both cell lines. Other drugs, including dopamine, paeonol, amiloride, and riluzole, showed no effect on [^{3}H]L-lysine uptake in both NSC-34 cell lines (Table 5).

Kinetics of drug-induced inhibition of [^{3}H]L-lysine uptake in NSC-34 cell lines

The Lineweaver–Burk plot for L-lysine uptake demonstrated that donepezil showed competitive inhibition with K_i values of 2.16 mM and 1.66 mM in the WT and MT cell lines, (Fig. 3A, 3E) respectively. Verapamil competitively inhibited [^{3}H]L-lysine uptake with K_i values of 1.13 mM in the WT cells and 0.399 mM in the MT cell line (Fig. 3B, 3F). Furthermore, quinidine showed competitive inhibition in the WT cell line with a Ki value of 0.94 mM (Fig. 3C) and non-competitive inhibition in the MT cell line with a Ki value of 2.01 mM (Fig. 3G). In addition, L-dopa showed un-competitive inhibition in the WT and MT cell lines with K_i values of 1.31 mM and 0.76 mM (Fig. 3D, 3H), respectively.

[^{3}H]L-Lysine uptake by NSC-34 ALS cells pretreated with glutamate and other pro-inflammatory cytokines

To examine the effect of glutamate toxicity and other pro-inflammatory cytokines, we evaluated the uptake of [^{3}H]L-lysine in NSC-34 cell lines. The WT cell line was treated 24 h prior to the uptake study with 500 μM glutamate, 20 ng/mL lipopolysaccharide (LPS), tumor necrosis factor (TNF-α), and 100 μM hydrogen peroxide (H_2O_2). In the WT cell line, [^{3}H]L-lysine uptake was significantly decreased in the presence of the above treatments, as shown in Fig. 4A. Similarly, in the MT cell line, the [^{3}H]L-lysine uptake decreased by 79% with glutamate, 80% with LPS, 64% with TNF-α, and 76% with H_2O_2 compared to that in the control. However, the addition of 10 mM L-lysine to these pretreated cells significantly increased the uptake in the MT cell line. All subsequent pre-incubations were conducted for 24 h under exposure to pro-inflammatory cytokines (Fig. 4B). Quantitative real-time PCR demonstrated similar results. The expression level of Slc7a1 mRNA in the MT cell line was lower after treatment with glutamate, LPS, TNF-α, and H_2O_2 compared to the corresponding levels in the control. In contrast, co-treatment with pro-inflammatory cytokines and L-lysine significantly increased the expression level of Slc7a1 mRNA, as shown in Fig. 4C. Collectively, our results demonstrated the neuroprotective effect of L-lysine in various pro-inflammatory states.

DISCUSSION

The purpose of this study was to explore alterations in the CAT-1 system and the effect of lysine on pro-inflammatory states in NSC-34 cell lines. On the basis of a prior study and our results, we evaluated the gene expression level of CAT-1 (Slc7a1), which is expressed in NSC-34 cell lines. In the siRNA transfection study, mRNA expression level and uptake of Slc7a1 siRNA were significantly reduced compared to that of the control siRNA in the NSC- 34 cell lines. Overall, these results suggest that [^{3}H]L-lysine is transported primarily by Slc7a1/system y^+ in the ALS cell-line model (Fig. 1). Previous studies have shown that the post-translational modification of lysine residues has been linked to mutations in SOD1 that are linked to ALS (Petrov *et al*., 2016). To achieve a clear understanding of the transporter involved in transport of L-lysine across NSC-34 cell lines, we evaluated the mRNA expression levels of Slc6a14/system $B^{0,+}$ and Slc7a9/system $b^{0,+}$; both

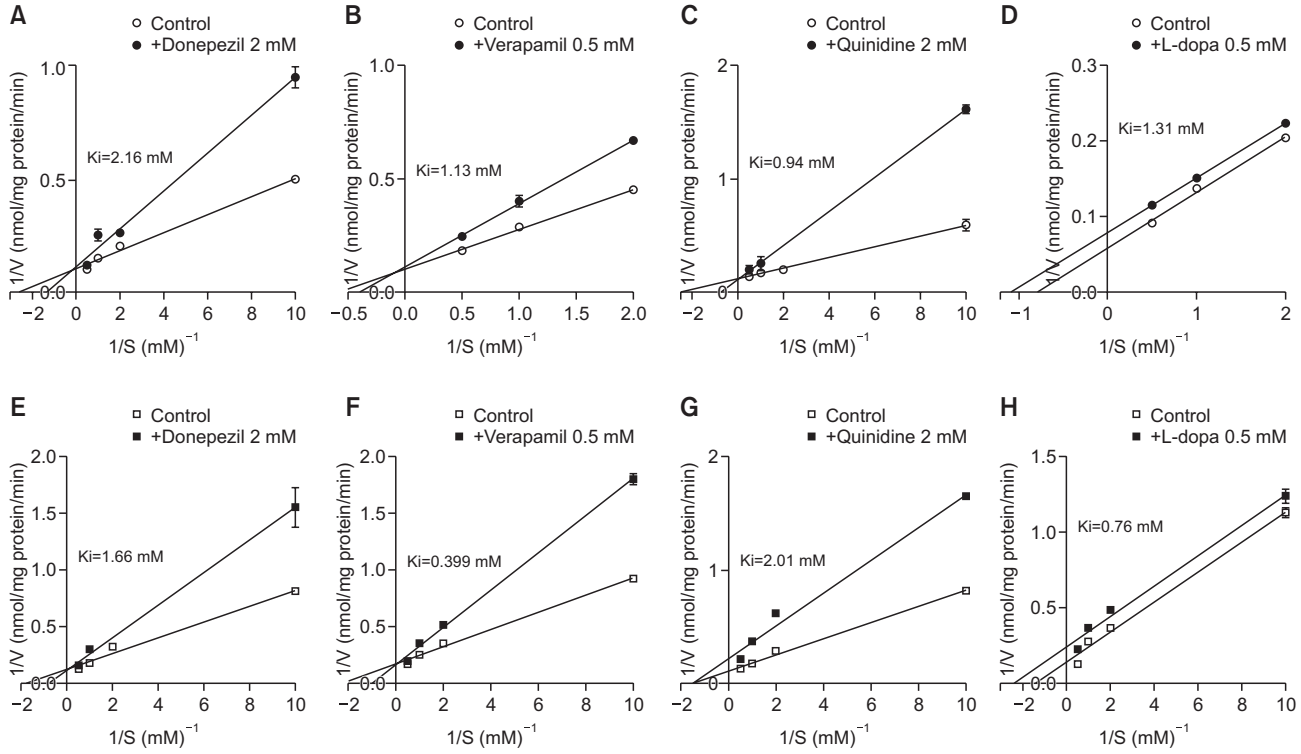

Fig. 3. Lineweaver–Burk plot for [^{3}H]L-lysine uptake by NSC-34 cell lines. [^{3}H]L-Lysine uptake was performed in the presence of 2 mM donepezil, 0.5 mM verapamil, 2 mM quinidine and 0.5 mM L-dopa or in their absence in WT (circle) and MT (square) cell lines at pH 7.4 and 37°C for 5 min. (A-D) shows inhibition with donepezil and verapamil, quinidine, and L-dopa in WT cell line, (E-H) shows inhibition in MT cell lines. The data represent the mean ± SEM (n=3-4).

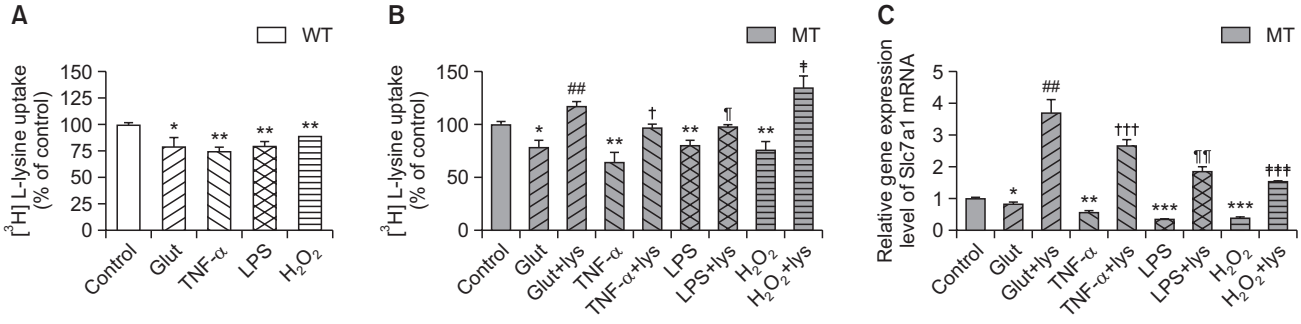

Fig. 4. Effect of pretreatment with glutamate and pro-inflammatory cytokines on [^{3}H]L-lysine uptake by NSC-34 cell lines. (A) WT cell line was exposed to 500 μM glutamate, 20 ng/mL TNF-α and LPS, and 100 μM H_2O_2 for 24 h. (B) [^{3}H]L-Lysine uptake in MT cell line pretreated with glutamate, TNF-α, LPS, and H_2O_2 with/without 10 mM L-lysine and incubated for 24 h. Uptake of [^{3}H]L-lysine was performed at pH 7.4 and 37°C for 5 min. Each value represents the mean ± SEM (n=3-4). $^{**}p$<0.01, $^{*}p$<0.05, significant difference vs control; $^{\#\#}p$<0.01, vs glutamate treatment; $^{\dagger}p$<0.05, vs TNF-α treatment; $^{\P}p$<0.01, vs LPS and $^{\ddagger}p$<0.01, vs H_2O_2 treatment. (C) Slc7a1 mRNA expression level in MT cell line. Each value represents the mean ± SEM (n=3-4). $^{***}p$<0.001, $^{**}p$<0.01, $^{*}p$<0.05, significant difference vs control; $^{\#\#}p$<0.01, vs glutamate, $^{\dagger\dagger\dagger}p$<0.001, vs TNF-α; $^{\P\P}p$<0.01, vs LPS treatment and $^{\ddagger\ddagger\ddagger}p$<0.001, vs H_2O_2 treatment.

were undetermined in the NSC-34 cell lines (data not shown). A preceding study has shown that the transport of CAA, such as arginine, is transported by both system y^+ and system y^+L (Bae *et al*., 2015). However, our data do not support that L-lysine is transported by system y^+L because L-lysine transport in NSC-34 cell lines is voltage sensitive (Table 1) and system y^+L is not voltage sensitive (O'Kane *et al*., 2006). In addition, in NSC-34 cell lines, [^{3}H]L-lysine transport is not inhibited by N-MM and strongly inhibited by NEM. Earlier studies have shown that NEM, which is a sulfhydryl reagent, inactivates the low-affinity lysine transporter system y^+ in human erythrocytes (Devés *et al*., 1998). The present study demonstrates that [^{3}H]L-lysine uptake was not significantly decreased in the absence of sodium in either cell line, as shown in Table 1; therefore, we hypothesized that transport of [^{3}H]L-lysine in NSC-34 cell lines is sodium-independent. Our result is consistent with previous

studies (Closs *et al*., 2006; O'Kane *et al*., 2006). Furthermore, in our study, strong inhibition of [^{3}H]L-lysine uptake was observed with homoarginine, N-MMA, NEM, and harmaline in both NSC-34 cell lines (Furesz *et al*., 1991), as presented in Table 2. These results suggest that L-lysine transport in ALS cell lines occurs through CAT-1 and that it may be related to system y^+ (O'Kane *et al*., 2006; Kim *et al*., 2008).

In our study, [^{3}H]L-lysine uptake was shown to be time- and concentration-dependent in NSC-34 cell lines; the uptake in the ALS cell-line model (MT) was lower than that in the normal (WT) cell line (Fig. 2, Table 3). The reduced uptake of L-lysine in MT cell lines might be due to mutation, deletion, or resistance of transporters, resulting in a lower transport activity as compared to that of the WT cell lines. Previous studies have reported similar results, as D-serine and PBA levels were decreased in MT cell lines of ALS (Lee *et al*., 2017; Gyawali and Kang, 2021b). These results are in agreement with a previous report indicating that the level of L-lysine is increased in the lumbar spinal cord of a mutant SOD^{G93A} model of ALS mice compared to that in WT mice (Jung *et al*., 2013). Furthermore, the uptake study in the presence of 2 mM solutions of various unlabeled amino acids showed that L-lysine, L-arginine, and L-ornithine, which are CAA and CAT-1 substrates, strongly inhibited the uptake of [^{3}H] L-lysine in both cell lines. L-Histidine showed weaker inhibition compared to CAA because it is largely unprotonated at pH 7.4, and L-leucine showed strong inhibition of [^{3}H] L-lysine uptake in NSC-34 cell lines (Tomi *et al*., 2009). However, choline and L-citrulline produced no effect on the uptake of [^{3}H]L-lysine (Table 4). This observation might be attributed to the fact that L-citrulline and choline follow different transport systems; L-citrulline has been shown to follow the LAT-1 transporter system (Lee and Kang, 2018).

Moreover, we investigated the effect of various drugs on the uptake of [^{3}H]L-lysine in an ALS cell-line model. Verapamil is a calcium channel blocker that has shown a neuroprotective effect in $SOD1^{G93A}$ mice (Zhang *et al*., 2019). In our study, it showed significant inhibition of the uptake of [^{3}H]L-lysine in the NSC-34 cell lines. Donepezil, an AChE inhibitor used in AD therapy (Kang *et al*., 2005), significantly inhibited the uptake in both cell lines. In addition, clonidine, quinidine, and gabapentin (an anticonvulsant drug) significantly reduced the uptake of [^{3}H]L-lysine in the NSC-34 cell lines (Table 5). Lineweaver–Burk plot analysis revealed the inhibitory effect of donepezil, verapamil, L-dopa, and quinidine. Donepezil and verapamil showed competitive inhibition in both NSC-34 cell lines. Our data show that the disease ALS model cell type is more sensitive to inhibition by donepezil and verapamil than the control WT cell lines. However, quinidine showed competitive inhibition in WT cell lines and non-competitive inhibition in the MT cell lines. The non-competitive inhibition in MT cell lines might be due to the alteration in the binding site in the disease model of ALS. L-Dopa showed uncompetitive inhibition in both cell lines. We hypothesized that both L-lysine and L-dopa follow different transporter systems (Kageyama *et al*., 2000) and that L-dopa binds to sites other than the L-lysine binding site and, therefore, did not show competitive inhibition (Fig. 3).

Pro-inflammatory toxic factors and other cytokines that are released from $SOD1^{G93A}$ astrocytes can trigger damage to motor neurons, as reported in previous studies (Lee *et al*. , 2016). In a previous study that evaluated the concentration-dependent effect of 0.25-1 mM glutamate in TR-BBB cells over a 24 h incubation period, cell viability significantly decreased with increasing glutamate concentration (Zhang *et al*., 2019). TNF-α plays a central role in microglial activation, neuronal excitotoxicity, and synapse loss. (Brohawn *et al*., 2016). LPS is a pro-inflammatory cytokine, and a previous study demonstrated the presence of A1-40/42 and LPS in amyloid plaques in the gray and white matter of AD brains (Zhan *et al*., 2016). In addition, H_2O_2, a product of the SOD1-catalyzed reaction at pathological concentrations of 10-100 μM, regulates the toxicity and misfolding of wild-type SOD1 and transitive-response DNA/RNA-binding protein 43 kDa (TDP-43) in neuronal cells (Ayers *et al*., 2016). Our results showed that pretreatment with glutamate, TNF-α, LPS, and H_2O_2 showed marked reduction in [^{3}H]L-lysine uptake in both cell lines (Fig. 4). We hypothesize that the alteration in the expression of transporters in the presence of pro-inflammatory cytokines might be the reason for the reduction in the uptake of [^{3}H]L-lysine. As reported in a previous article, depending on the cell type, there is up- and down-regulation of transporter expression in the inflammatory state (Gyawali and Kang, 2021a). However, in the MT cell lines, co-treatment with L-lysine had a protective effect against pro-inflammatory cytokine states. The neuroprotective effect of L-lysine has been demonstrated in previous work on intracerebral hemorrhage-injured mice (Cheng *et al*., 2020).

Our study demonstrates that the alteration in the transport of L-lysine in ALS model cell lines and transport of lysine is mediated mainly by system y^+ in the WT and MT cell lines. The system showed higher affinity and lower capacity in disease model cell lines than the control cell line. Lysine produced a restorative effect in the presence of inflammatory cytokines in the mutant SOD^{G93A} cell lines model of ALS.

ACKNOWLEDGMENTS

This work was supported by a National Research Foundation of Korea (NRF) grant funded by the Korean government (MSIT) (No. 2019R1F1A1044048) (YSK).

REFERENCES

Adachi, Y., Ono, N., Imaizumi, A., Muramatsu, T., Andou, T., Shimodaira, Y., Nagao, K., Kageyama, Y., Mori, M., Noguchi, Y., Hashizume, N. and Nukada, H. (2018) Plasmaamino acid profile in severely frail elderly patients in Japan. *Int. J. Gerontol.* **12**, 290-293.

Ayers, J. I., Fromholt, S. E., O'Neal, V. M., Diamond, J. H. and Borchelt, D. R. (2016) Prion-like propagation of mutant SOD1 misfolding and motor neuron disease spread along neuroanatomical pathways. *Acta Neuropathol.* **131**, 103-114.

Bae, S. Y., Xu Q., Hutchinson, D. and Colton, C. A. (2015) Y^+ and y^+ L arginine transporters in neuronal cells expressing tyrosine hydroxylase. *Biochim. Biophys. Acta* **1745**, 65-73.

Bahri, S., Curis, E., El Wafi, F. Z., Aussel, C., Chaumeil, J. C., Cynober, L. and Zerrouk, N. (2008) Mechanisms and kinetics of citrulline uptake in a model of human intestinal epithelial cells. *Clin. Nutr.* **27**, 872-880.

Brohawn, D. G., O'Brien, L. C. and Bennett, J. P., Jr. (2016) RNAseq analyses identify tumor necrosis factor-mediated inflammation as a major abnormality in ALS spinal cord. *PLoS ONE* **11**, e0160520.

Cashman, R. N., Durham, H. D., Blusztajn, K. J., Oda, K., Tabira, T., Shaw, T. I., Dahrouge, S. and Antel, P. J. (1992) Neuroblastoma x spinal cord (NSC) hybrid cell lines resemble developing motor neurons. *Dev. Dyn.* **194**, 209-221.

Cheng, J., Tang, J. C., Pan, M. X., Chen, S. F., Zhao, D., Zhang, Y., Liao, H. B., Zhuang, Y., Lei, R. X., Wang, S., Liu, A. C., Chen, J.,

Zhang, Z. H., Li, H. T., Wan, Q. and Chen, Q. X. (2020) L-Lysine confers neuroprotection by suppressing inflammatory response via microRNA-575/PTEN signaling after mouse intracerebral hemorrhage injury. *Exp. Neurol.* **327**, 113214.

Closs, E. I., Biossel, J. P., Habermerier, A. and Rotmann, A. (2006) Structure and function of cationic amino acid transporters (CATs). *J. Membr. Biol.* **213**, 67-77.

Closs, E. I., Simon, A., Vékony, N. and Rotmann, A. (2004) Plasma membrane transporters for arginine. *J. Nutr.* **134**, 2752S-2759S.

Devés, R., Angelo, S. and Chavez, P. (1993) N-ethylmaleimide discriminates between two lysine transport systems in human erythrocytes. *J. Physiol.* **468**, 753-766.

Devés, R. and Boyd, C. A. (1998) Transporters for cationic amino acids in animal cells: discovery, structure, and function. *Physiol. Rev.* **78**, 487-545.

Furesz, T. C., Moe, A. J. and Smith, C. H. (1991) Two cationic amino acid transport systems in human placental basal plasma membranes. *Am. J. Physiol.* **261**, C246-C252.

Gyawali, A., Gautam, S., Hyeon, S. J., Ryu, H. and Kang, Y. S. (2021) L-citrulline level and transporter activity are altered in experimental models of amyotrophic lateral sclerosis. *Mol. Neurobiol.* **58**, 647-657.

Gyawali, A. and Kang, Y. S. (2019) Blood-to-retina transport of imperatorin involves the carrier-mediated transporter system at the inner blood-retinal barrier. *J. Pharm. Sci.* **108**, 1619-1626.

Gyawali, A. and Kang, Y. S. (2021a) Pretreatment effect of inflammatory stimuli and characteristics of tryptophan transport on brain capillary endothelial (TR-BBB) and motor neuron like (NSC-34) cell lines. *Biomedicines* **9**, 9.

Gyawali, A. and Kang, Y. S. (2021b) Transport alteration of 4-phenyl butyric acid mediated by a sodium- and proton-coupled monocarboxylic acid transporter system in ALS model cell lines (NSC-34) under inflammatory states. *J. Pharm. Sci.* **110**, 1374-1384.

Iłzecka, J., Stelmasiak, Z., Solski, J., Wawrzycki, S. and Szpetnar, M. (2003) Plasma amino acids concentration in amyotrophic lateral sclerosis patients. *Amino Acids* **25**, 69-73.

Jung, M. K., Kim, K. Y., Lee, N. Y., Kang, Y. S., Hwang, Y. J., Kim, Y., Sung, J. J., Mckee, A., Kowall, N., Lee, J. and Ryu, H. (2013) Expression of taurine transporter (TauT) is modulated by heat shock factor 1 (HSF1) in motor neurons of ALS. *Mol. Neurobiol.* **47**, 699-710.

Kageyama, T., Nakamura, M., Matsuo, A., Yamasaki, Y., Takakura, Y., Hashida, M., Kanai, Y., Naito, M., Tsuruo, T., Minato, N. and Shimohama, S. (2000) The 4F2hc/LAT1 complex transports L-DOPA across the blood-brain barrier. *Brain Res.* **879**, 115-121.

Kang, Y. S., Lee, K., Lee, N. Y. and Terasaki, T. (2005) Donepezil, tacrine and α-phenyl-n-tert-butyl nitrone (PBN) inhibit choline transport by conditionally immortalized rat brain capillary endothelial cell lines (TR-BBB). *Arch. Pharm. Res.* **28**, 443-450.

Kim, C. S., Cho, S. H., Chun, H. S., Lee, S. Y., Endou, H., Kanai, Y. and Kim, D. K. (2008) BCH, an inhibitor of system L amino acid transporters, induces apoptosis in cancer cells. *Biol. Pharm. Bull.* **31**, 1096-1100.

Lee, J., Hyeon, S. J., Im, H., Ryu, H., Kim, Y. and Ryu, H. (2016) Astrocytes and microglia as non-cell autonomous players in the pathogenesis of ALS. *Exp. Neurobiol.* **25**, 233-240.

Lee, N. Y. and Kang, Y. S. (2016) *In vivo* and *in vitro* evidence for brain uptake of 4-phenylbutyrate by the monocarboxylate transporter 1 (MCT1). *Pharm. Res.* **33**, 1711-1722.

Lee, N. Y., Kim, Y., Ryu, H. and Kang, Y. S. (2017) The alteration of serine transporter activity in a cell line model of amyotrophic lateral sclerosis (ALS). *Biochem. Biophys. Res. Commun.* **483**, 135-141.

Lee, K. E. and Kang, Y. S. (2018) L-Citrulline restores nitric oxide level and cellular uptake at the brain capillary endothelial cell line (TR-BBB cells) with glutamate cytotoxicity. *Microvasc. Res.* **120**, 29-35.

Mitsuoka, K., Shirasaka, Y., Fukush, I. A., Sato, M., Nakamura, T., Nakanishi, T. and Tamai, I. (2009) Transport characteristics of L-citrulline in renal apical membrane of proximal tubular cells. *Biopharm. Drug Dispos.* **30**, 126-137.

O'Kane, L. R., Viña, J. R., Simpson, I., Zaragozá, R., Mokashi, A. and Hawkins, R. A. (2006) Cationic amino acid transport across the blood-brain barrier is mediated exclusively by system y^+. *Am. J. Physiol. Endocrinol. Metab.* **291**, E412-E419.

Patten, B. M., Harati, Y., Acosta, L., Jung, S. S. and Felmus, T. M. (1978) Free amino acid levels in amyotrophic lateral sclerosis. *Ann. Neurol.* **3**, 305-309.

Petrov, D., Daura, X. and Zagrovic, B. (2016) Effect of oxidative damage on the stability and dimerization of superoxide dismutase 1. *Biophys. J.* **110**, 1499-1509.

Rasouli, S., Abdolvahabi, A., Croom, C. M., Plewman, D. L., Shi, Y., Ayers, J. I. and Shaw, B. F. (2017) Lysine acylation in superoxide dismutase-1 electrostatically inhibits formation of fibrils with prion-like seeding. *J. Biol. Chem.* **292**, 19366-19380.

Rojas, F., Gonzalez, D., Cortes, N., Ampuero, E., Hernández, D. E., Fritz, E., Abarzua, S., Martinez, A., Elorza, A. A., Alvarez, A., Court, F. and van Zundert, B. (2015) Reactive oxygen species trigger motoneuron death in non-cell-autonomous models of ALS through activation of c-Abl signaling. *Front. Cell. Neurosci.* **9**, 203.

Rowland, L. P. and Shneider, N. A. (2001) Amyotrophic lateral sclerosis. *N. Engl. J. Med.* **344**, 1688-1700.

Tomi, M., Kitade, N., Hirose, S., Yokota, N., Akanuma, S., Tachikawa, M. and Hosoya, K. (2009) Cationic amino acid transporter 1-mediated L-arginine transport at the inner blood-retinal barrier. *J. Neurochem.* **111**, 716-725.

Ukmar-Godec, T., Hutten, S., Grieshop, M. P., Rezaei-Ghaleh, N., Cima-Omori, M. S., Biernat, J., Mandelkow, E., Soding, J., Dormann, D. and Zweckstetter, M. (2019) Lysine/RNA-interactions drive and regulate biomolecular condensation. *Nat. Commun.* **10**, 2909.

Van Winkle, L. J., Campione, A. L. and Farrington, B. H. (1990) Development of system B0,+ and a broad-scope Na(+)-dependent transporter of zwitterionic amino acids in preimplantation mouse conceptuses. *Biochim. Biophys. Acta* **1025**, 225-233.

Wee, C. Y., Yap, P. T. and Shen, D.; Alzheimer's Disease Neuroimaging Initiative (2013) Prediction of alzheimer's disease and mild cognitive impairment using cortical morphological patterns. *Hum. Brain Mapp.* **34**, 3411-3425.

Zhan, X., Stamova, B., Jin, L. W., DeCarli, C., Phinney, B. and Sharp, F. R. (2016) Gram-negative bacterial molecules associate with Alzheimer disease pathology. *Neurology* **87**, 2324-2332.

Zhang, X., Chen, S., Lu, K., Wang, F., Deng, J., Xu, Z., Wang, X., Zhou, Q., Le, W. and Zhao, Y. (2019) Verapamil ameliorates motor neuron degeneration and improves lifespan in the $SOD1^{G93A}$ mouse model of ALS by enhancing autophagic flux. *Aging Dis.* **10**, 1159-1173.